Acta Crystallographica Section D
Biological Crystallography
ISSN 0907-4449

A new pentameric structure of rotavirus NSP4 revealed by molecular replacement

Anita R. Chacko,[a] J. Jeyakanthan,[b] G. Ueno,[c] K. Sekar,[d] C. Durga Rao,[e] Eleanor J. Dodson,[f] Kaza Suguna[a]* and Randy J. Read[g]*

[a]Molecular Biophysics Unit, Indian Institute of Science, C. V. Raman Avenue, Bangalore, Karnataka 560 012, India, [b]Department of Bioinformatics, Alagappa University, Karaikudi 630 003, India, [c]Division of Synchrotron Radiation Instrumentation, Riken SPring-8 Center, 1-1-1 Kuoto, Sayo, Hyogo 678-5148, Japan, [d]Bioinformatics Centre, Indian Institute of Science, C. V. Raman Avenue, Bangalore, Karnataka 560 012, India, [e]Department of Microbiology and Cell Biology, Indian Institute of Science, C. V. Raman Avenue, Bangalore, Karnataka 560 012, India, [f]Department of Chemistry, York Structural Biology Laboratory, University of York, Heslington, York YO10 5YW, England, and [g]Department of Haematology, University of Cambridge, Cambridge Institute of Medical Research, Wellcome Trust, MRC Building, Hills Road, Cambridge CB2 2XY, England

Correspondence e-mail: suguna@mbu.iisc.ernet.in, rjr27@cam.ac.uk

Received 4 October 2011
Accepted 21 November 2011

PDB Reference: rotavirus NSP4, 3miw.

The region spanning residues 95–146 of the rotavirus nonstructural protein NSP4 from the asymptomatic human strain ST3 has been purified and crystallized and diffraction data have been collected to a resolution of 2.6 Å. Several attempts to solve the structure by the molecular-replacement method using the available tetrameric structures of this domain were unsuccessful despite a sequence identity of 73% to the already known structures. A more systematic approach with a dimer as the search model led to an unexpected pentameric structure using the program *Phaser*. The various steps involved in arriving at this molecular-replacement solution, which unravelled a case of subtle variation between different oligomeric states unknown at the time of solving the structure, are presented in this paper.

1. Introduction

The 175-amino-acid nonstructural protein 4 (NSP4) of rotavirus has been identified as the first virus-encoded enterotoxin (Ball *et al.*, 1996; Tian *et al.*, 1996). It is a multifunctional protein, with most of its properties being associated with the C-terminal cytoplasmic tail of approximately 131 amino acids. It is essential for rotavirus replication, transcription, morphogenesis and pathogenesis (Silvestri *et al.*, 2005; López *et al.*, 2005). NSP4 acts as the intracellular receptor for the double-layered particles and transports them from the cytoplasm to the ER lumen, where assembly of the mature particles takes place (Au *et al.*, 1993; Chan *et al.*, 1988; O'Brien *et al.*, 2000; Taylor *et al.*, 1993). NSP4 occurs in multiple forms: endoplasmic reticulum-resident (Bergmann *et al.*, 1989; Chan *et al.*, 1989), cytoplasmic membrane-anchored (Storey *et al.*, 2007), and proteolytically cleaved and secreted (Zhang *et al.*, 2000; Bugarcic & Taylor, 2006), as well as oligomeric and high-molecular-weight forms (Maass & Atkinson, 1990; Taylor *et al.*, 1992; Jagannath *et al.*, 2006). The diverse properties associated with NSP4 include membrane destabilization (Newton *et al.*, 1997; Tian *et al.*, 1996), diarrhoea induction (Ball *et al.*, 1996; Horie *et al.*, 1999), calcium binding (Estes *et al.*, 2001), intracellular calcium mobilization (Tian *et al.*, 1994; Dong *et al.*, 1997), inhibition of sodium absorption by activation of TMEM16A (Ousingsawat *et al.*, 2011), viroporin activity (Hyser *et al.*, 2010), VP4 binding (Estes *et al.*, 2001; Hyser *et al.*, 2008), inhibition of the microtubule-mediated secretory pathway (Xu *et al.*, 2000), alteration of actin network organization (Berkova *et al.*, 2007), induction of calcium-regulated and viroplasm-associated vesicular compartments (Berkova *et al.*, 2006), and interaction with extracellular proteins such as laminin $\beta3$ and fibronectin (Boshuizen *et al.*, 2004), integrins $\alpha1\beta1$ and $\alpha2\beta1$ (Seo *et al.*, 2008), calnexin (Mirazimi *et al.*, 1998), tubulin (Xu *et al.*, 2000) and caveolin (Parr *et al.*, 2006;

Mir *et al.*, 2007). Recently, we have reported that the optimal properties of the protein are dependent on a unique conformation which appears to be effected by cooperation between the N- and C-terminal regions of the cytoplasmic tail (Jagannath *et al.*, 2006). All of these studies reveal the structural and functional complexities of the protein.

Efforts in several laboratories to crystallize the complete C-terminal cytoplasmic region have not been successful. To date, only the crystal structures of a synthetic peptide from residues 95 to 137 (Bowman *et al.*, 2000) and the biologically expressed region from amino acids 95 to 146 (Deepa *et al.*, 2004, 2007) are available. The flexible region of about 40 residues from the C-terminus appears to hinder crystallization of the complete C-terminal cytoplasmic tail. NSP4:95–146 represents the largest region that could be crystallized to date and the last nine residues in this peptide could not be traced in the electron-density map (Deepa *et al.*, 2004, 2007). The region 95–137 of NSP4 in these three structures was found to form a tetrameric coiled-coil domain.

Rotavirus infections can be symptomatic or asymptomatic depending on the virus and the host. However, an analysis of NSP4 sequences from a large number of symptomatic and asymptomatic strains did not reveal any amino acid or motif that is consistently associated with the virulence of the virus in the animal host or the diarrhoea-inducing ability of the purified protein in the newborn mouse model system (Lin & Tian, 2003; Jagannath *et al.*, 2000). Significantly, the region between amino acids 135 and 141 exhibits a high degree of sequence variation and mutations in this interspecies-variable domain (ISVD) have been observed to affect the virulence of the virus as well as the diarrhoea-inducing and double-layered particle-binding activities of the protein (Zhang *et al.*, 1998; Jagannath *et al.*, 2006). Recent studies have indicated that the biological properties of NSP4 are dependent on a unique conformation and that mutations in either the N-terminal or the C-terminal regions or the ISVD significantly affect its properties (Jagannath *et al.*, 2006). With a view to obtaining insights into the structural variation in the C-terminal region and its correlation with biological activity among different NSP4s, we have been analyzing the structures of NSP4:95–146 from different rotavirus strains that show variation in sequence in this region. In this study, we have initiated structure analysis of NSP4:95–146 from the asymptomatic human rotavirus strain ST3. While the previously reported structures of this domain from two different strains of the virus, namely simian SA11 and human asymptomatic I321 (Deepa *et al.*, 2007), could easily be determined by molecular replacement using the tetrameric model of the synthetic peptide (PDB entry 1g1j; Bowman *et al.*, 2000), structure solution of the present example turned out to be quite challenging.

The way in which the molecular-replacement solutions from the program *Phaser* were examined and improved, starting with a dimeric search model and ultimately revealing a totally unanticipated pentamer, is described in this paper.

2. Materials and methods

2.1. Cloning, expression and purification

A DNA fragment of NSP4 from the G4P[6] asymptomatic human strain ST3 corresponding to residues 95–146 (Fig. 1) was amplified from the NSP4ΔN72 cDNA clone (Jagannath *et al.*, 2006) using strain-specific and position-specific primers. The GenBank accession number of NSP4 from ST3 is U59110. The forward primer contained sites for *Eco*RI and *Nde*I restriction endonucleases and the reverse primer contained a termination codon and a site for *Hin*dIII. The *Eco*RI and *Hin*dIII PCR fragment was first cloned in a pBluescript KS+ (pBS) vector. The *Nde*I–*Hin*dIII fragment liberated from pBS was then cloned into pET-22b(+) between the same sites. The protein is expressed without a histidine tag, but contains an additional methionine at the N-terminus. The gene sequence was verified by nucleotide-sequence analysis (Macrogen, Republic of Korea). The deletion-mutant protein expressed in *Escherichia coli* BL21 (DE3) was highly soluble and was purified as described previously (Deepa *et al.*, 2007). Briefly, the induced bacterial cells were lysed by sonication in a buffer consisting of 10 m*M* sodium acetate pH 5.6, 100 m*M* NaCl, 0.1 m*M* EDTA, 3 m*M* PMSF and then mixed with 1% NP40. The NSP4 protein from the lysate was precipitated in 40% ammonium sulfate and partially purified by anion-exchange chromatography using a Mono-Q column followed by size fractionation on a HiPrep 26/60 Sephacryl S-200 column (GE Healthcare) using 20 m*M* Tris–HCl pH 7.5 buffer containing 100 m*M* NaCl. The protein in the peak fractions was concentrated to 30–40 mg ml^{-1} using Centricon-10 microconcentrators (Millipore). The purity and integrity of the protein was determined using MALDI mass spectrometry as well as tricine–sodium dodecyl sulfate–polyacrylamide gel electrophoresis (Tricine–SDS–PAGE).

2.2. Crystallization

Purified ST3 NSP4:95–146 was crystallized at 293 K by the hanging-drop vapour-diffusion method by mixing 2 µl protein solution at a concentration of approximately 30 mg ml^{-1} and 2 µl reservoir solution. Initial screening was carried out using Crystal Screen, Crystal Screen 2 and Index from Hampton Research (Jancarik *et al.*, 1991). Small crystals were observed in three different conditions all at pH 6.5. The best crystals appeared in Crystal Screen 2 condition No. 23, consisting of 10%(*v*/*v*) dioxane, 0.1 *M* MES pH 6.5 and 1.6 *M* ammonium sulfate. In further trials, the protein

	95		110	120	130		146
SA11	IEKQM	DRVVKEMRRQ	LEMIDKLTTR	EIEQVELLKR	IYDKLTVQTTG	EIDMTK	
I321	IE**T**QM	DRVVKEMRRQ	LEMIDKLTTR	EIEQVELLKR	IYDKLTV**R**T**AD**	EIDMTK	
ST3	IE**Q**QM	DR**I**VKEMRRQ	LEMIDKLTTR	EIEQ**I**ELLKR	I**H**D**N**L**ITRPVN**	**V**IDM**SM**	

Figure 1
Sequence alignment of NSP4:95–146 from the SA11, I321 and ST3 strains of rotavirus. Residues that differ from those in the protein from the ST3 strain are shown in bold.

concentration was increased to 40 mg ml^{-1} and the drop ratio was modified. Larger crystals of dimensions 0.3 × 0.25 × 0.1 mm were obtained within two weeks (Fig. 2).

2.3. Data collection

Crystals of NSP4:95–146 from ST3 were transferred into a cryoprotectant consisting of 10%(*v*/*v*) ethylene glycol, kept sealed over reservoir solution containing mother liquor and 10% ethylene glycol for 10 min and then flash-cooled in liquid nitrogen. The data were collected with a MAR CCD 225 detector using X-rays of wavelength 1.0 Å on BL26B2 at the SPring-8 synchrotron in Japan. A total of 180° of data were collected with an oscillation angle of 1°. The crystal-to-detector distance was 184 mm. The data were indexed, integrated and scaled using *DENZO* and *SCALEPACK* from the *HKL*-2000 suite (Otwinowski & Minor, 1997). Table 1 gives the data-collection statistics.

2.4. Computations

Molecular-replacement calculations were carried out using the programs *AMoRe* (Navaza, 2001), *Phaser* (McCoy *et al.*, 2007), *MOLREP* (Vagin & Teplyakov, 1997, 2010), *Queen of Spades* (Glykos, 2005) and *EPMR* (Kissinger *et al.*, 1999).

3. Results and discussion

The crystals of NSP4:95–146 from ST3 belonged to space group $P4_22_12$, with unit-cell parameters $a = b = 63.33$, $c = 122.87$ Å. As three structures that are approximately 73% identical in sequence to the newly crystallized construct are available [PDB entries 1g1j (a synthetic peptide of SA11 NSP4:95–136; Bowman *et al.*, 2000), 2o1j (NSP4:95–146 from I321; Deepa *et al.*, 2007) and 2o1k (NSP4:95–146 from SA11; Deepa *et al.*, 2007)], we attempted to solve the structure by molecular replacement. We used the tetramer, a four-helical coiled-coil structure, found in the three previously reported structures as

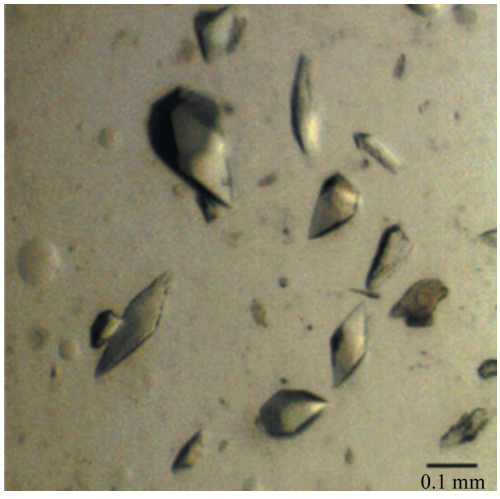

Figure 2
Crystals of NSP4:95–146 from the asymptomatic human strain ST3 of rotavirus.

Table 1
Crystal data and data-collection statistics.

Values in parentheses are for the highest resolution shell.

Temperature (K)	100
Space group	$P4_22_12$
Unit-cell parameters (Å)	
a	63.33
b	63.33
c	122.87
Matthews coefficient V_M (Å^3 Da^{-1})	1.9
Solvent content (%)	35.2
No. of molecules in asymmetric unit	1 pentamer
Resolution range (Å)	50–2.6 (2.69–2.60)
Observed reflections	100818 (7545)
No. of unique reflections	8158 (785)
Completeness (%)	97.7 (96.4)
Multiplicity	12.4 (9.4)
$\langle I/\sigma(I)\rangle$	30.99 (4.14)
R_{merge} (%)†	5.5 (20.0)

† $R_{merge} = \sum_{hkl}\sum_i |I_i(hkl) - \langle I(hkl)\rangle| / \sum_{hkl}\sum_i I_i(hkl)$, where $I_i(hkl)$ is the *i*th observation of reflection *hkl* and $\langle I(hkl)\rangle$ is the weighted average intensity for all observations of reflection *hkl*.

the search model. The Matthews coefficient of 2.4 Å^3 Da^{-1} (Matthews, 1968) indicated the presence of a single molecule of the size of a tetramer in the asymmetric unit (the corresponding value for a pentamer is 1.9 Å^3 Da^{-1}). Since no solution was obtained using the tetramer, we also attempted MR using a dimer and a monomer. Different resolution ranges were tried in order to arrive at a solution. MR was also attempted in the lower symmetry space groups from *P*422 to *P*2, suspecting a case of pseudosymmetry, but no solution was obtained. For *Phaser* solutions the *Z* score was always less than 5 and LLG was negative. In *AMoRe*, the best solutions had correlation coefficients of less than 50 and *R* factors between 0.55 and 0.60 and could not be refined further. Solutions from *EPMR* and *Queen of Spades* had similar *R* factors. *MOLREP* also resulted in solutions with *R* factors in the region of 0.60 and low scores of about 3.4. Thus, no solutions were obtained with a search for a tetrameric model.

A more systematic approach was subsequently performed. The various steps involved in the search are shown in Fig. 3 and described here. (i) A dimer (*AB*) of the synthetic peptide (PDB entry 1g1j) was used as the input model to the program *Phaser* (McCoy *et al.*, 2007) and a search was performed for two copies of this dimer for space groups in the point group *P*422. Two solutions were obtained in space group $P4_22_12$, related by a register shift of one dimer along the coiled-coil axis; the better of these had a translation-function *Z* score (TFZ) of 8.1 and an LLG score of 97. (ii) The two dimers (*AB* and *CD*) formed a tetramer superficially similar to that found in the synthetic peptide, but with a gap on one side between monomers *A* and *D*. (iii) Each of the four monomers was omitted one at a time to identify the set of three monomers with the highest LLG value. (iv) When the best-fitting three monomers (*B*, *C* and *D*) were used as a single-entity input model and a search was carried out for another monomer, two families of solutions appeared: one in which (iv*a*) the additional monomer appeared at the position of the monomer *A* that was deleted and another (iv*b*) in the gap between *A* and *D*.

(v) Adding these two monomers to the other three made the model a pentamer, which gave an LLG score (251) that was substantially higher than that for the best tetramer solution (LLG = 162 if the asymmetric unit is assumed to contain a pentamer instead of a tetramer).

However, the pentamer did not appear to be completely symmetric. The best of the five monomers, *B*, was once again chosen by the criterion of which one caused the greatest drop in the LLG score when omitted from the model. A symmetric pentamer was generated from five copies of the *B* chain by working out the best fivefold NCS operators to superimpose the pentamer on itself (*e.g. BCDEA* on *ABCDE*, *BCDEA* on *CDEAB etc.*). The LLG score improved considerably when this pentamer was refined as five rigid bodies (LLG = 361). Rigid-body refinement with this model in *REFMAC*5 resulted in an *R* factor of 0.39 and an $R_{\rm free}$ of 0.51. Following the procedure of Keller *et al.* (2006), many cycles of DM phase extension from 5 Å with fivefold NCS averaging were carried out, which resulted in a model with an *R* factor of 0.29 and an $R_{\rm free}$ of 0.42. The electron-density maps calculated at this stage were clear and interpretable. Residues 95–135 could be modelled in all five chains, but the C-terminal ten residues were not visible in the maps, as in the case of the tetrameric structures, indicating that this region is also highly flexible in the pentameric structure. After several cycles of model building, addition of solvent molecules and corrections for data anisotropy, twinning and pseudo-symmetry, the refinement converged at an *R* factor of 0.27 and an $R_{\rm free}$ of 0.31 in space group $P4_2$. A detailed description of the refinement will be published elsewhere.

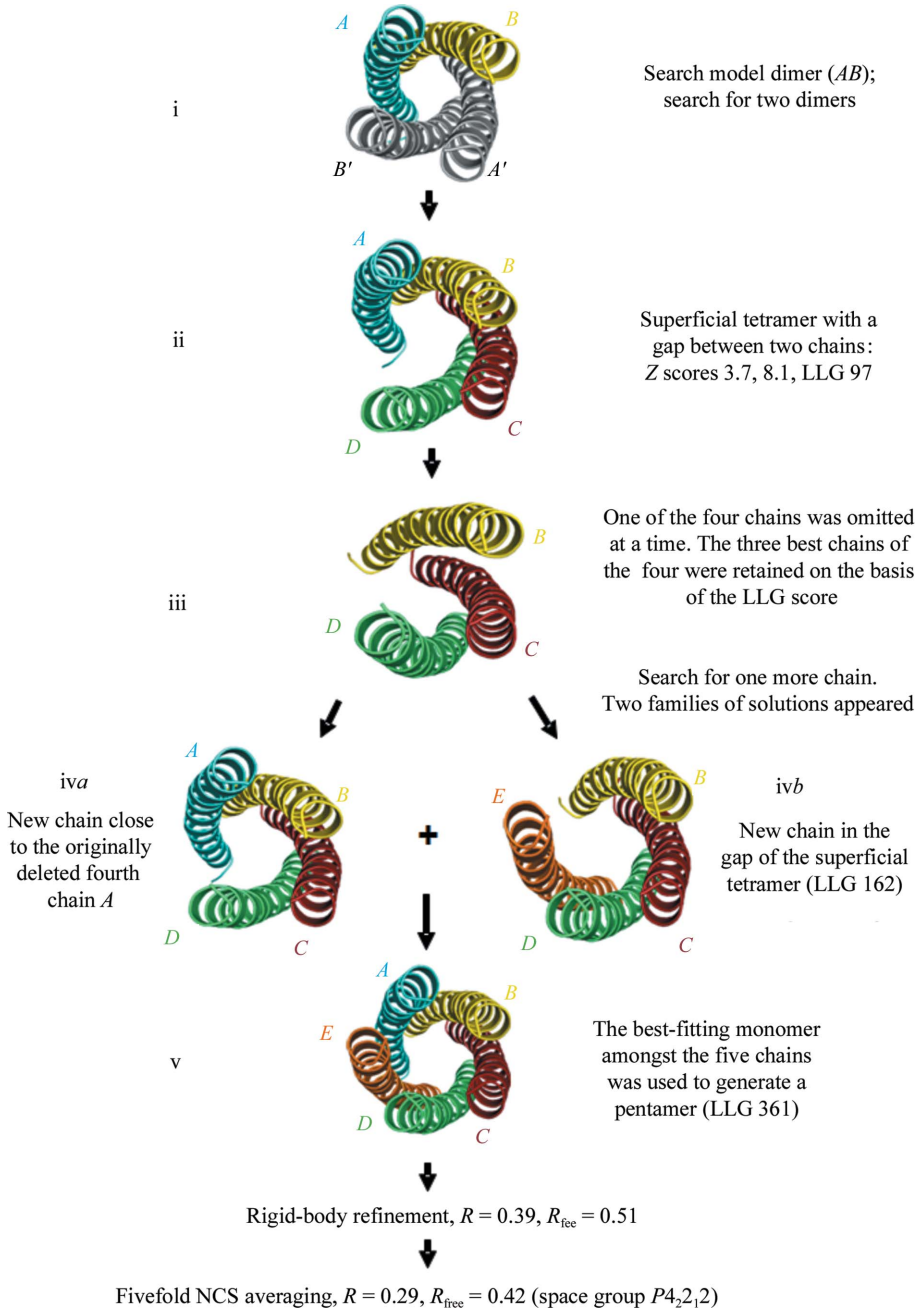

Figure 3
Various steps in the detection of a pentamer starting with a dimer from a tetrameric structure.

Self-rotation function maps were calculated initially to find inter-chain relationships. However, no detectable peaks were observed. The maps were re-examined after structure solution, but as the fivefold axis is approximately parallel to the *c* axis (the direction cosines of the fivefold axis are −0.10, 0.17 and −0.98), the self-rotation peaks around $\kappa = 72^\circ$ were found to be masked by the peaks that correspond to the crystallographic fourfold axis along the *c* axis.

The structure of the rotavirus NSP4 being a pentamer is a novel and a completely unanticipated result. This result provides new insights into the structural and functional diversity of NSP4 and the significance of structural variations in its biological functions and gives a new direction to the work on NSP4. As mentioned earlier, all three of the previously reported structures are tetramers. Interestingly, the tetrameric arrangement in these structures is not a result of a strict fourfold rotation axis. A rotation of 81° relates two chains and the other two chains are generated by a twofold rotation of these two chains. In the synthetic peptide and NSP4:95–146 from SA11 the twofold axis is a crystallographic axis, whereas in NSP4:95–146 from I321 it is a noncrystallographic axis. The angle of 81° being exactly between the angles of perfect fourfold and fivefold rotations might indicate the flexibility of the chains to form different types of oligomers, which

could result in functional differences among different NSP4 proteins.

This particular case study once again proves the power of the molecular-replacement method/program. There are many instances in which the method has been unsuccessful because of small differences between the initial model and the actual structure. However, in this study the search model comprises only two-fifths of the scattering matter and also deviates significantly from the final structure (rotation angle of 81° for the search model compared with 72° for the resultant pentamer) and yet it was possible to obtain the solution by carefully examining the solution peaks and carefully building the entire molecule. If difficulties are encountered while attempting molecular replacement with partial models, it may be worthwhile scrutinizing the results with manual intervention at intermediate stages and improving the solutions gradually. Although MR has become a simple method to arrive at a solution, its importance cannot be underestimated and it can still yield surprises at every turn.

This work was supported by the Structural Genomics programme under the Genomics Initiative at the Indian Institute of Science funded by the Department of Biotechnology (DBT). The Drug and Molecular Design program of the DBT supported the mass-spectrometry facility. Financial support from the Indian Council of Medical Research is acknowledged. Preliminary data were collected at the X-ray Facility for Structural Biology at the Molecular Biophysics Unit of the Indian Institute of Science. ARC acknowledges the University Grants Commission (UGC), Government of India for the award of a fellowship. ARC acknowledges CCP4 for the help extended to attend the CCP4 Study Weekend at Reading (2007), which provided fruitful discussions on MR.

References

Au, K. S., Mattion, N. M. & Estes, M. K. (1993). *Virology*, **194**, 665–673.

Ball, J. M., Tian, P., Zeng, C. Q.-Y., Morris, A. P. & Estes, M. K. (1996). *Science*, **272**, 101–104.

Bergmann, C. C., Maass, D., Poruchynsky, M. S., Atkinson, P. H. & Bellamy, A. R. (1989). *EMBO J.* **8**, 1695–1703.

Berkova, Z., Crawford, S. E., Blutt, S. E., Morris, A. P. & Estes, M. K. (2007). *J. Virol.* **81**, 3545–3553.

Berkova, Z., Crawford, S. E., Trugnan, G., Yoshimori, T., Morris, A. P. & Estes, M. K. (2006). *J. Virol.* **80**, 6061–6071.

Boshuizen, J. A., Rossen, J. W., Sitaram, C. K., Kimenai, F. F., Simons-Oosterhuis, Y., Laffeber, C., Büller, H. A. & Einerhand, A. W. (2004). *J. Virol.* **78**, 10045–10053.

Bowman, G. D., Nodelman, I. M., Levy, O., Lin, S. L., Tian, P., Zamb, T. J., Udem, S. A., Venkataraghavan, B. & Schutt, C. E. (2000). *J. Mol. Biol.* **304**, 861–871.

Bugarcic, A. & Taylor, J. A. (2006). *J. Virol.* **80**, 12343–12349.

Chan, W. K., Au, K. S. & Estes, M. K. (1988). *Virology*, **164**, 435–442.

Chan, R. C., Tam, J. S., Fok, T. F. & French, G. L. (1989). *J. Hosp. Infect.* **13**, 367–375.

Deepa, R., Durga Rao, C. & Suguna, K. (2007). *Arch. Virol.* **152**, 847–859.

Deepa, R., Jagannath, M. R., Kesavulu, M. M., Durga Rao, C. & Suguna, K. (2004). *Acta Cryst.* D**60**, 135–136.

Dong, Y., Zeng, C. Q.-Y., Ball, J. M., Estes, M. K. & Morris, A. P. (1997). *Proc. Natl Acad. Sci. USA*, **94**, 3960–3965.

Estes, M. K., Kang, G., Zeng, C. Q.-Y., Crawford, S. E. & Ciarlet, M. (2001). *Novartis Found. Symp.* **238**, 82–96.

Glykos, N. M. (2005). *J. Appl. Cryst.* **38**, 574–575.

Horie, Y., Nakagomi, O., Koshimura, Y., Nakagomi, T., Suzuki, Y., Oka, T., Sasaki, S., Matsuda, Y. & Watanabe, S. (1999). *Virology*, **262**, 398–407.

Hyser, J. M., Collins-Pautz, M. R., Utama, B. & Estes, M. K. (2010). *mBio*, **1**, e00265-10.

Hyser, J. M., Zeng, C. Q.-Y., Beharry, Z., Palzkill, T. & Estes, M. K. (2008). *Virology*, **373**, 211–228.

Jagannath, M. R., Kesavulu, M. M., Deepa, R., Sastri, P. N., Kumar, S. S., Suguna, K. & Rao, C. D. (2006). *J. Virol.* **80**, 412–425.

Jagannath, M. R., Vethanayagam, R. R., Reddy, B. S., Raman, S. & Rao, C. D. (2000). *Arch. Virol.* **145**, 1339–1357.

Jancarik, J., Scott, W. G., Milligan, D. L., Koshland, D. E. & Kim, S.-H. (1991). *J. Mol. Biol.* **221**, 31–34.

Keller, S., Pojer, F., Heide, L. & Lawson, D. M. (2006). *Acta Cryst.* D**62**, 1564–1570.

Kissinger, C. R., Gehlhaar, D. K. & Fogel, D. B. (1999). *Acta Cryst.* D**55**, 484–491.

Lin, S. L. & Tian, P. (2003). *Virus Gen.* **26**, 271–282.

López, T., Camacho, M., Zayas, M., Nájera, R., Sánchez, R., Arias, C. F. & López, S. (2005). *J. Virol.* **79**, 184–192.

Maass, D. R. & Atkinson, P. H. (1990). *J. Virol.* **64**, 2632–2641.

Matthews, B. W. (1968). *J. Mol. Biol.* **33**, 491–497.

McCoy, A. J., Grosse-Kunstleve, R. W., Adams, P. D., Winn, M. D., Storoni, L. C. & Read, R. J. (2007). *J. Appl. Cryst.* **40**, 658–674.

Mir, K. D., Parr, R. D., Schroeder, F. & Ball, J. M. (2007). *Virus Res.* **126**, 106–115.

Mirazimi, A., Nilsson, M. & Svensson, L. (1998). *J. Virol.* **72**, 8705–8709.

Navaza, J. (2001). *Acta Cryst.* D**57**, 1367–1372.

Newton, K., Meyer, J. C., Bellamy, A. R. & Taylor, J. A. (1997). *J. Virol.* **71**, 9458–9465.

O'Brien, G. J., Bryant, C. J., Voogd, C., Greenberg, H. B., Gardner, R. C. & Bellamy, A. R. (2000). *Virology*, **270**, 444–453.

Otwinowski, Z. & Minor, W. (1997). *Methods Enzymol.* **276**, 307–326.

Ousingsawat, J., Mirza, M., Tian, Y., Roussa, E., Schreiber, R., Cook, D. I. & Kunzelmann, K. (2011). *Pflugers Arch.* **461**, 579–589.

Parr, R. D., Storey, S. M., Mitchell, D. M., McIntosh, A. L., Zhou, M., Mir, K. D. & Ball, J. M. (2006). *J. Virol.* **80**, 2842–2854.

Seo, N.-S., Zeng, C. Q.-Y., Hyser, J. M., Utama, B., Crawford, S. E., Kim, K. J., Höök, M. & Estes, M. K. (2008). *Proc. Natl Acad. Sci. USA*, **105**, 8811–8818.

Silvestri, L. S., Tortorici, M. A., Vasquez-Del Carpio, R. & Patton, J. T. (2005). *J. Virol.* **79**, 15165–15174.

Storey, S. M., Gibbons, T. F., Williams, C. V., Parr, R. D., Schroeder, F. & Ball, J. M. (2007). *J. Virol.* **81**, 5472–5483.

Taylor, J. A., Meyer, J. C., Legge, M. A., O'Brien, J. A., Street, J. E., Lord, V. J., Bergmann, C. C. & Bellamy, A. R. (1992). *J. Virol.* **66**, 3566–3572.

Taylor, J. A., O'Brien, J. A., Lord, V. J., Meyer, J. C. & Bellamy, A. R. (1993). *Virology*, **194**, 807–814.

Tian, P., Ball, J. M., Zeng, C. Q.-Y. & Estes, M. K. (1996). *J. Virol.* **70**, 6973–6981.

Tian, P., Hu, Y., Schilling, W. P., Lindsay, D. A., Eiden, J. & Estes, M. K. (1994). *J. Virol.* **68**, 251–257.

Vagin, A. & Teplyakov, A. (1997). *J. Appl. Cryst.* **30**, 1022–1025.

Vagin, A. & Teplyakov, A. (2010). *Acta Cryst.* D**66**, 22–25.

Xu, A., Bellamy, A. R. & Taylor, J. A. (2000). *EMBO J.* **19**, 6465–6474.

Zhang, M., Zeng, C. Q.-Y., Dong, Y., Ball, J. M., Saif, L. J., Morris, A. P. & Estes, M. K. (1998). *J. Virol.* **72**, 3666–3672.

Zhang, M., Zeng, C. Q.-Y., Morris, A. P. & Estes, M. K. (2000). *J. Virol.* **74**, 11663–11670.